



The Society shall not be responsible for statements or opinions advanced in papers or in discussion at meetings of the Society or of its Divisions or Sections, or printed in its publications. Discussion is printed only if the paper is published in an ASME Journal. Papers are available from ASME for fifteen months after the meeting.  
Printed in USA.

## New Materials for Fabricated Gas Turbine Hot Section Components

M. F. ROTHMAN and C. R. PATRIARCA  
Haynes International, Inc  
P.O. Box 9013  
Kokomo, IN 46902-9013

### ABSTRACT

Materials have been developed in recent years which are particularly well-suited for use in fabricated gas turbine hot section components. Among these are HAYNES<sup>®</sup> alloy No. 230 and HASTELLOY<sup>®</sup> alloy S. These alloys combine very good performance characteristics with capability for fabrication into such complex components as combustion chambers, afterburner flameholders, seal rings, and thermocouple/probe assemblies. The properties and fabrication characteristics of these two materials are reviewed and compared with other well-known gas turbine alloys.

### INTRODUCTION

Two of the principal driving forces behind the development of new alloys for gas turbine components have always been (1) the quest for ever-higher temperature/strength performance characteristics, and (2) the desire to achieve greater component reliability and longer service life. For components fabricated

from sheet, plate and bar stock, alloy designers must also take care to provide for the formability and joinability of newly developed materials.

As a class, solid-solution-strengthened superalloys offer a carefully tailored balance of properties to achieve both the required service capabilities, and ready fabrication into complex parts. It is in this class of gas turbine materials that several alloys have evolved which provide for significant design/performance advantages over more traditional alloys. Among these are HAYNES alloy No. 230, a Ni-Cr-W alloy, and HASTELLOY alloy S, a Ni-Cr-Mo material.

The chemical compositions of these alloys are given in Table 1, together with the compositions of the key reference materials to which alloy No. 230 and alloy S will be compared. The design and performance characteristics of all of these materials will be reviewed first. This will be followed by an examination of the specific fabrication characteristics of the alloys, including both forming and welding.

Table 1

### NOMINAL COMPOSITIONS OF ALLOYS

	Weight Percent										
	Ni	Co	Fe	Cr	Mo	W	C	La	Mn	Si	Others
HAYNES alloy No. 188	22	Bal.	3*	22	--	14	0.10	0.03	1.25*	0.35	--
HAYNES alloy No. 230	Bal.	3*	3*	22	2	14	0.10	0.02	0.5	0.4	0.3 Al
HASTELLOY alloy S	Bal.	2*	3*	16	15	--	0.02*	0.02	0.65	0.50	0.3 Al
HASTELLOY alloy X	Bal.	1.5	18.5	22	9	0.6	0.10	--	1.0*	1.0*	--
Alloy No. 625	Bal.	1*	5*	22	9	--	0.10*	--	0.50*	0.50*	3.7 Cb+Ta
* Maximum											0.4* Al, 0.4*Ti

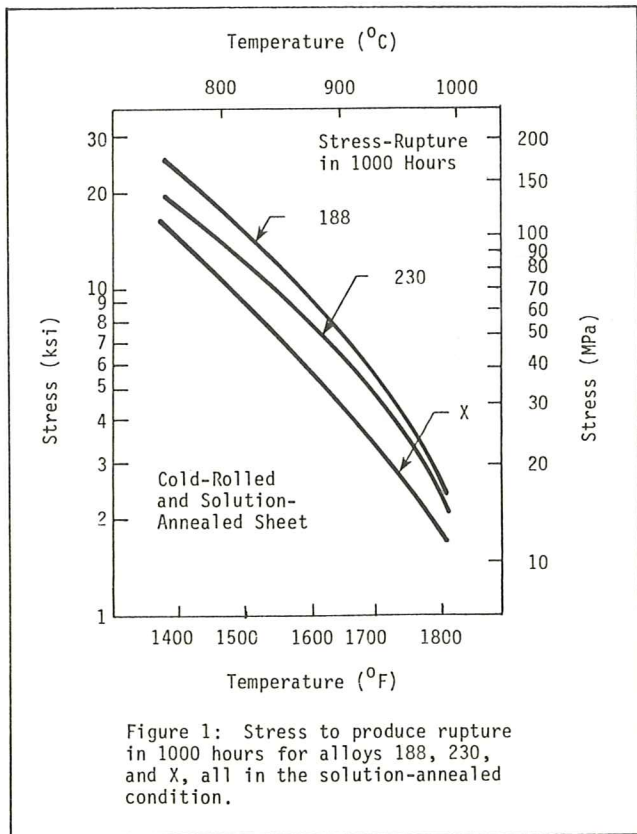
HAYNES and HASTELLOY are registered trademarks of Cabot Corporation

ALLOY PERFORMANCE CHARACTERISTICS

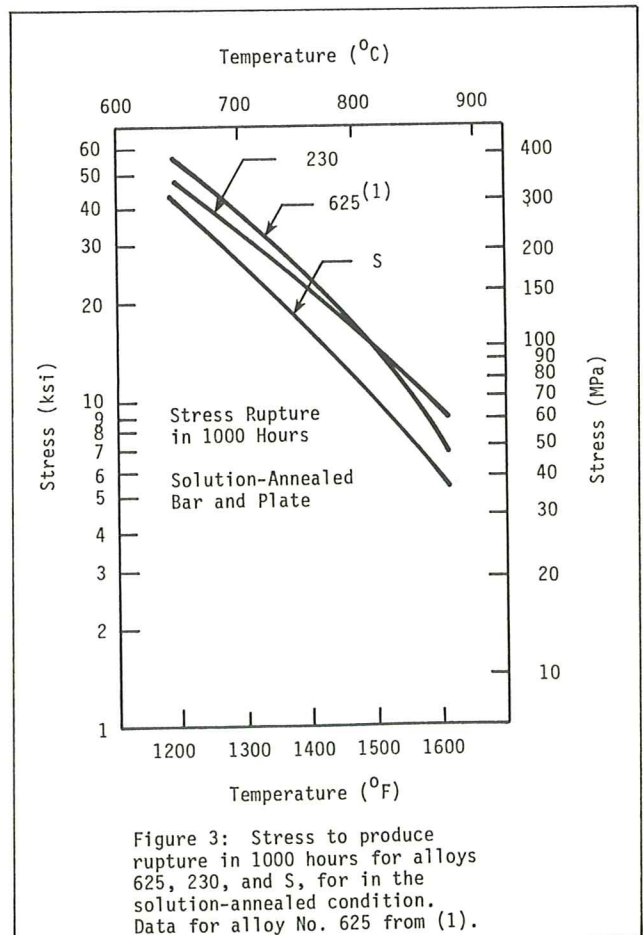
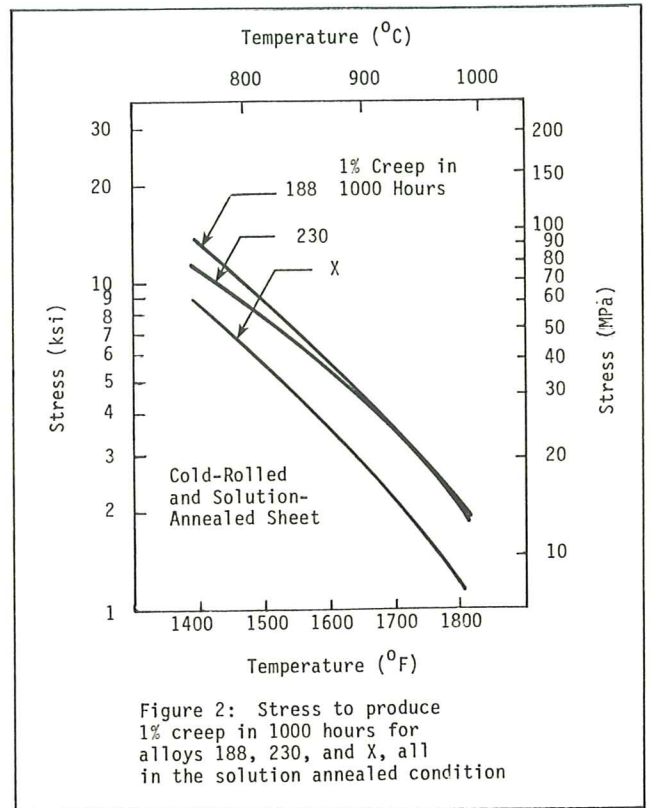
Creep and Stress-Rupture Strength

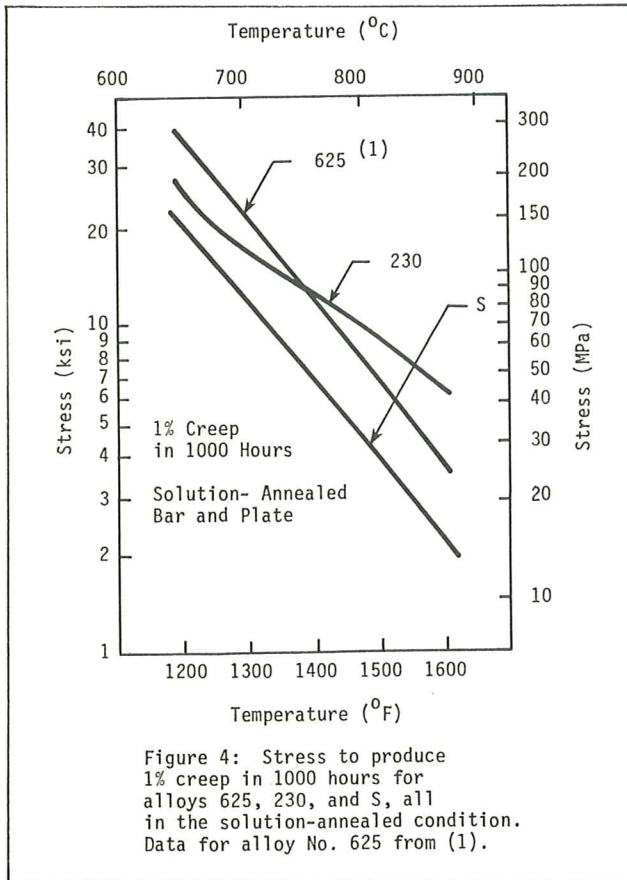
Solid-solution-strengthened superalloys are often employed for components subject to high-temperature/low-stress conditions, where creep and stress-rupture strength are important performance criteria. The temperature range of interest is nominally about 1200°F to 2000°F (650°C to 1095°C), although temperatures above and below this range are certainly relevant. The higher end of the range is the regime for combustor cans, transition liners and afterburner components. Lower temperatures are pertinent to seal rings, casings and tail pipes, among others.

A comparison of the typical stress-rupture properties of alloy No. 230 sheet product at 1400°F to 1800°F (760°C to 980°C) to those for HAYNES alloy No. 188 and HASTELLOY alloy X is shown in Figure 1. These latter two materials represent the upper and lower limits, respectively, for the strength characteristics of typical conventional burner can materials. A similar comparison for 1% creep strength at 1400°F to 1800°F (760°C to 980°C) is shown in Figure 2. As may be discerned from the two figures, alloy No. 230 exhibits strength intermediate between alloys X and No. 188, approaching that of alloy No. 188 at temperatures above 1600°F (870°C).



Similar stress-rupture and 1% creep strength comparisons between alloy No. 230, alloy S and alloy No. 625 plate and bar materials are shown in Figures 3 and 4, respectively, for the temperature





range of 1200°F to 1600°F (650°C to 870°C). The data for alloy No. 625 are taken from Moon et al<sup>(1)</sup>. Alloy No. 625 exhibits high strength in the temperature regime of 1200°F to 1400°F (650°C to 760°C) as a consequence of in-service Ni<sub>3</sub>Cb precipitation strengthening. The strengthening advantage is diminished in the 1400°F to 1600°F (760°C to 870°C) range, where the Ni<sub>3</sub>Cb precipitate overages rapidly, and alloy No. 230 becomes the stronger material. Alloy S is about 100°F (55°C) lower than alloy No. 625 in strength capability over the entire range of temperature, but as is discussed in the next section, it enjoys a considerable advantage in thermal stability over alloy No. 625.

Thermal Stability

Many materials exhibit excellent ductility when first placed into service; however, a key consideration in the performance and repairability of gas turbine hot section components is the maintenance of reasonable alloy ductility after long-term service exposure. Another important consideration for some components is retention of impact strength. A comparison of the response of key alloys to 8000-hour exposures at several intermediate temperatures is presented in Figure 5, which shows residual room-temperature tensile elongation for exposed plate samples. A similar comparison for impact strength at room temperature is given in Table 2.

While alloy S is not particularly strong in comparison to the other materials, it exhibits the

important advantage of high ductility and impact strength retention. Alloy No. 188, alloy No. 625 and alloy X all exhibit deleterious phase reactions as a consequence of exposure at 1200°F to 1600°F (650°C to 870°C). In addition to carbide precipitation, there is mu and sigma phase precipitation in alloy X, laves phase precipitation in alloy No. 188, and Ni<sub>3</sub>Cb (orthorhombic structure) needle phase formation in alloy No. 625.<sup>(2)</sup>

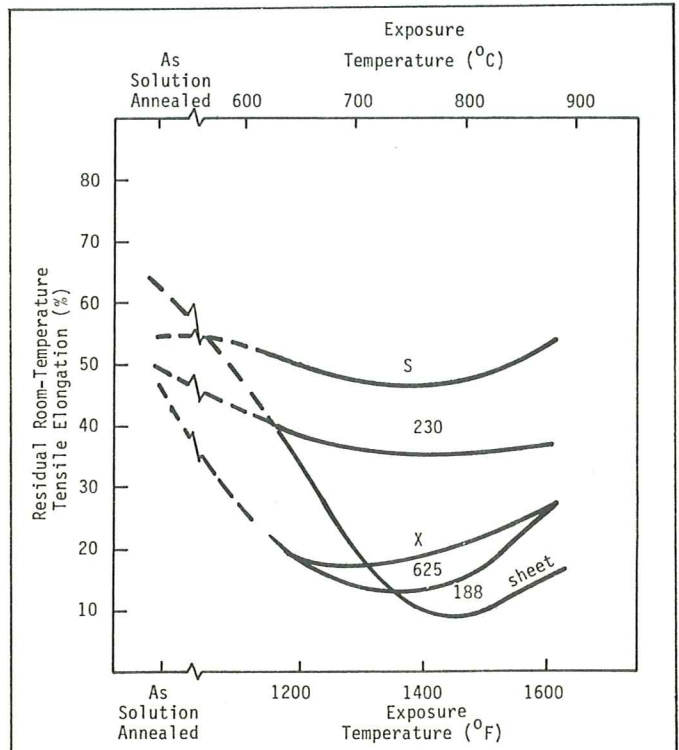


Figure 5: Room-temperature tensile elongation of plate material subjected to 8000 hour exposure at elevated temperature.

Alloy No. 230 exhibits perhaps the best combination of strength and thermal stability. Only carbide precipitation is observed with long-term thermal exposures. Although its levels of ductility and impact strength retention are lower than those for alloy S, they are still significantly higher than those for alloys X, No. 188 and No. 625.

Table 2

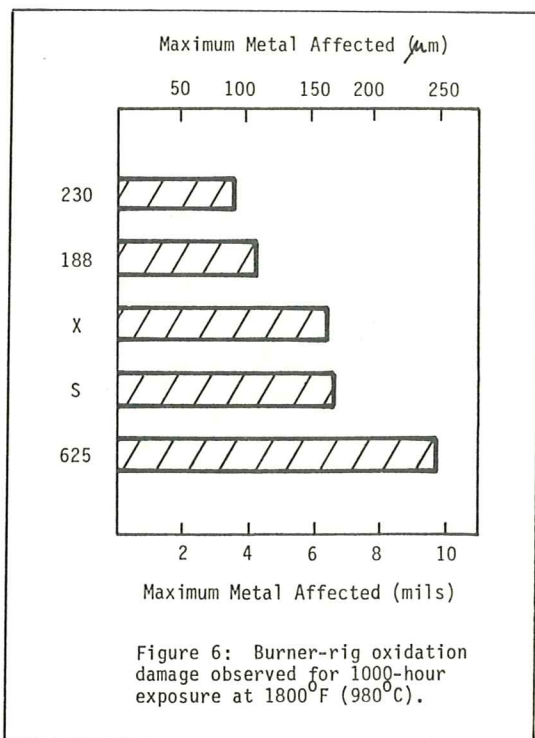
Residual Room-Temperature Impact Strength For Alloys Exposed at Temperature for 8000 Hours

Alloy	Solution-Annealed Charpy V-Notch Impact, Ft-Lb (Joules)	Charpy V-notch Impact Following Exposure at Temperature, Ft-Lb (Joules)		
		1200°F (650°C)	1400°F (760°C)	1600°F (870°C)
S	140 (190)	54 (73)	48 (65)	105 (142)
230	60 (82)	30 (41)	21 (29)	21 (29)
625	81 (110)	5 (7)	5 (7)	15 (20)
X	54 (73)	15 (20)	8 (11)	15 (20)
188	143 (194)	--	--	10 (14)

## Environment-Resistance

The stated temperature range of interest for the application of these materials reaches well into that regime wherein resistance to oxidation and turbine combustion gas environments is of great importance. Particularly in combustors, transition liners, and afterburner hardware, but in many of the less-demanding components as well, environmental degradation can play a key role in limiting component life.

The resistance of materials to turbine combustion gas environments is usually determined in burner rig tests. Results from such tests conducted at 1800°F (980°C) are shown in Figure 6.

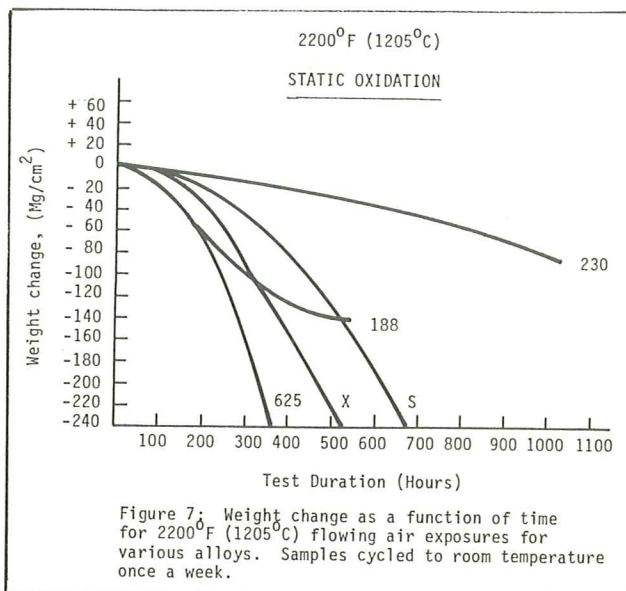


These results were generated for 1000-hour exposures in a Mach 0.3 burner rig with a 50:1 air:fuel ratio and cycling to less than 400°F (200°C) every 30 minutes by removal from the flame tunnel and forced-air cooling. Maximum metal affected was determined by metallographic assessment of both metal loss and maximum internal depth of penetration.

Alloys No. 230 and No. 188 behaved best in this test, with alloy No. 230 marginally the better of the two. Alloys X and S exhibited intermediate performance. Alloy No. 625 was the least resistant of the five materials examined, sustaining almost three times as much damage as that for alloy No. 230.

The superior resistance to oxidation of alloy No. 230 is evident at higher temperatures as well. Exposures to flowing air at temperatures as high as 2200°F (1205°C) have been performed for 1000 hours. Results of weight change measurements for the 2200°F (1205°C) exposures are shown in Figure 7. Alloys No. 625, X and S all show a tendency towards catastrophic weight loss per unit area well

before the 1000-hour tests were completed. The non-parabolic behavior of alloy No. 188 in the test is explained by the observation of massive internal oxidation of the sample for that material. Alloy No. 230, although not capable of sustained application at this temperature, still exhibits far better resistance to oxidation than any of the other materials evaluated.



Another form of possible high-temperature environmental degradation which is relevant to combustion chamber and transition liner performance is carburization. It is recognized that combustion under low-oxygen conditions can produce sooting, with heavy deposit buildup on metal surfaces. Resulting carburization can severely impair material performance in terms both of mechanical properties and of resistance to oxidation. It has been reported previously (3) that alloy No. 230 exhibits less sensitivity to increased oxidation damage under sooting conditions than alloys No. 188 or X. Unfortunately, similar data are not available for alloys S and No. 625.

In lieu of such data, results of carburization tests conducted at 1800°F (980°C) for 55 hours in a highly reducing gas mixture of Ar-5% H<sub>2</sub>-5% CO-5% CH<sub>4</sub> are presented in Table 3. Carbon absorption per unit area during the exposure was calculated from the change in carbon content, determined by chemical analysis, and a knowledge of the original specimen weight and surface area exposed. These results would suggest that the behavior of alloy S under sooting conditions might be better than alloy No. 230. Alloy No. 625, on the other hand, appears much more susceptible to carburization, and might therefore be expected to perform worse than the other four materials.

Table 3  
Carburization-Resistance of Alloys

Alloy	Carbon Absorption for 55-Hour Exposures in 1800°F (980°C) Carburizing Gas * (mg/cm <sup>2</sup> )
S	2.1
230	2.5
X	2.5
188	2.7
625	5.3

\*Ar-5%H<sub>2</sub>-5%CO-5%CH<sub>4</sub>

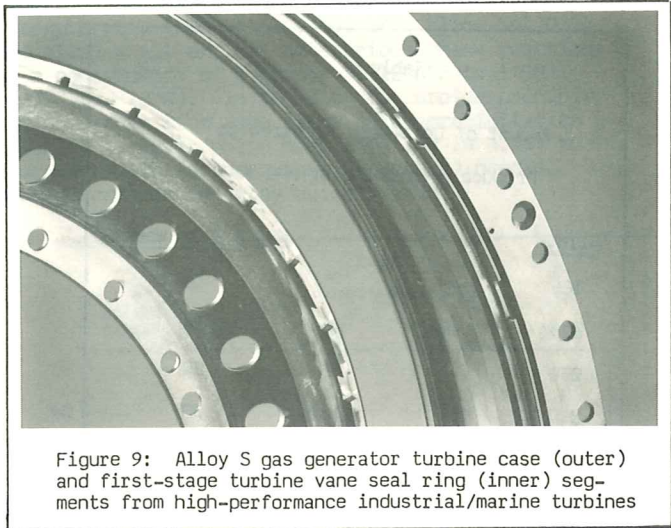


Figure 9: Alloy S gas generator turbine case (outer) and first-stage turbine vane seal ring (inner) segments from high-performance industrial/marine turbines

Mechanical Forming Characteristics

As a guide to the forming and shaping characteristics of the several alloys of interest, sheet samples 0.070-0.133 inches (1.8-3.4 mm) in thickness were subjected to cold-rolling reductions of up to 50%, with subsequent hardness and tensile property measurements. Nickel and cobalt-base alloys work harden to significantly higher hardness levels than do stainless steels. This is shown clearly in Figure 10. Based upon an arbitrary hardness limit of, say Rockwell C35, the amount of cold-work allowable for the various materials would be as given in Table 4.

ALLOY FABRICATION CHARACTERISTICS

Various sophisticated turbine components have been fabricated from all of the materials discussed here. Examples of fabrications involving the newer compositions, alloys No. 230 and S, are presented in Figures 8 and 9.

Figure 8 shows a combustor can for Avco Lycoming Textron's AGT 1500 engine fabricated from alloy No. 230 by Stolper Industries. This component was manufactured using heavy sheet metal, welded and brazed to form the final configuration shown.

Figure 9 shows segments of two components fabricated using alloy S. The outer ring is a gas generator turbine case, and the inner unit is a first stage vane seal ring. Both are used in industrial/marine gas turbine engines, and are manufactured from bar using a variety of forming and joining techniques.

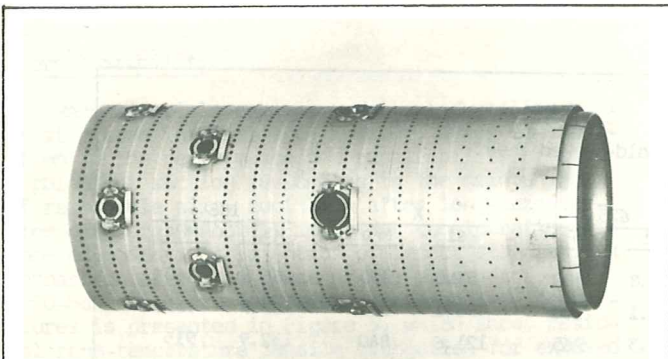


Figure 8: Alloy No. 230 combustor can for Avco Lycoming Textron AGT 1500 engine, fabricated by Stolper Industries.

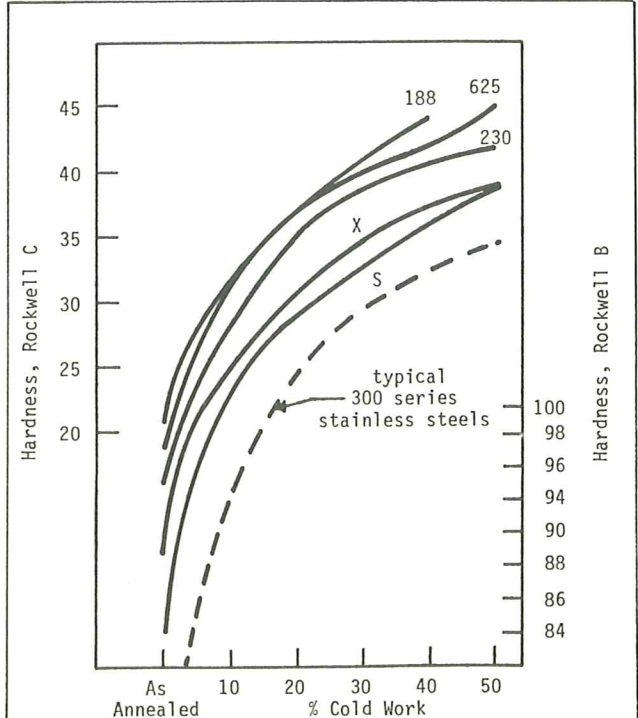


Figure 10: Hardness of sheet materials as a function of applied cold work.

Table 4

Amount of Cold-Work Required to  
Produce a Hardness of HRC 35

Alloy	% Cold Work
188	16
625	16
230	20
X	30
S	37

Hardness, however, is certainly not the only factor involved in establishing the limits to the amount of cold-work which can be imposed upon an alloy. A graph of the room-temperature tensile elongations measured as a function of amount of imposed cold-work for the five materials is presented in Figure 11. Similarly-measured room-temperature yield strengths are reported in Table 5. These data show that the four nickel-base alloys display similar residual tensile ductilities after cold working. Despite its higher hardness, alloy No. 188 exhibits significantly higher residual tensile elongation than that for the nickel-base materials after equivalent cold-work.

In terms of the yield strengths produced by cold working, the data in Table 5 indicate that alloy No. 625 requires the most applied stress to deform, and alloy X the least. Alloys S, No. 230 and No. 188 fall between these two, in increasing order of required stress to deform.

Summarizing the results of the as-cold-worked property evaluations, it is apparent that the responses to cold-work for alloy S and alloy No. 230 are similar to those for the more established materials. Alloy S is almost equivalent to alloy X in behavior, while alloy No. 230 is perhaps slightly easier to form than alloy No. 625.

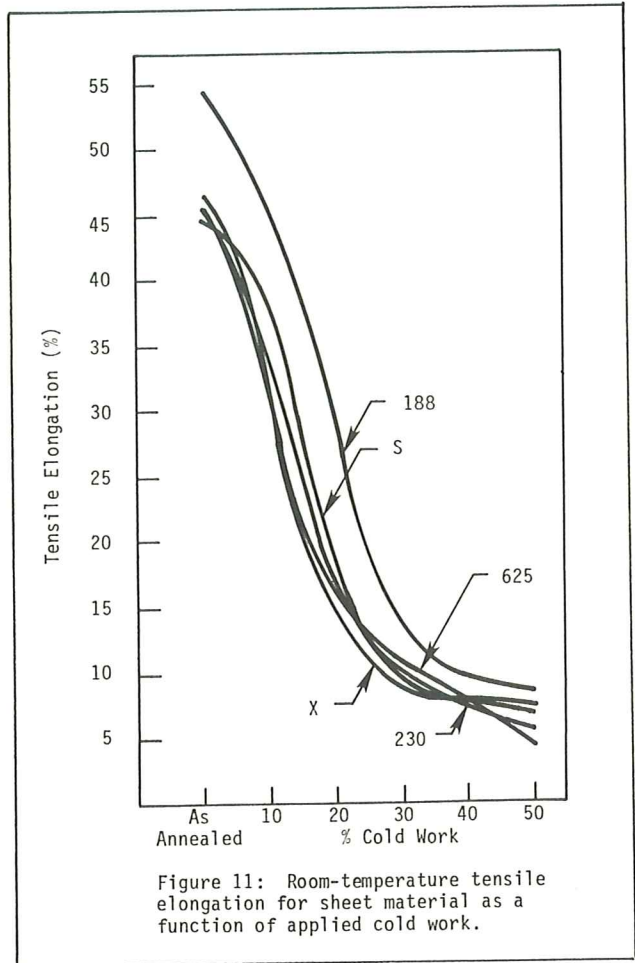


Figure 11: Room-temperature tensile elongation for sheet material as a function of applied cold work.

In the special case of drawability, similar behavior is observed. Table 6 contains comparative Olsen Cup Depth data for the alloys. These results, the averages of three or more tests, were generated using petroleum jelly as a lubricant. Here, alloy S performs better than the other alloys. Alloy No. 230 once again is slightly more drawable than alloy No. 625.

Table 5

0.2% Yield Strength of Cold-Worked Sheet

% Cold-Work	S		230		625		X		188	
	ksi	MPa	ksi	MPa	ksi	MPa	ksi	MPa	ksi	MPa
0	73.7	510	61.8	425	69.8	480	57.0	395	66.9	460
10	92.3	635	104.0	715	113.1	780	96.1	665	105.9	730
20	135.9	935	133.9	925	140.3	965	121.6	840	132.9	915
30	153.8	1060	160.1	1105	161.6	1115	142.2	980	167.0	1150
40	166.0	1145	172.6	1190	178.3	1230	158.7	1095	176.8	1220
50	177.1	1220	184.6	1275	192.9	1330	170.9	1180	-	-

Table 6  
Comparative Olsen Cup Depths

Alloy	Olsen Cup Depth	
	Inches	mm
S	.513	13.0
188	.490	12.4
X	.484	12.3
230	.460	11.7
625	.440	11.2

Table 7  
Room-Temperature Tensile Elongation  
For Cold Work and Re-annealed Sheet \*

Condition	Tensile Elongation (%)				
	S	230	625	X	188
As-solution annealed	44.5	46.6	45.7	45.8	54.2
40% C. W.	8.2	7.5	7.6	8.4	9.8
40% C. W. + 1750°F (955°C)	40.9	-	-	-	-
40% C. W. + 1850°F (1010°C)	43.0	-	41.8	32.3	-
40% C. W. + 1950°F (1065°C)	44.8	33.3	42.2	35.1	39.8
40% C. W. + 2050°F (1120°C)	51.2	35.5	44.2	36.6	43.2
40% C. W. + 2150°F (1175°C)	-	38.1	54.9	47.9	55.5
40% C. W. + 2250°F (1230°C)	-	47.2	-	-	62.1

\* 5 minute reanneal

Response to Annealing

Many forming operations will require multiple steps to complete finished components. A knowledge of the material response to intermediate annealing is important in establishing appropriate procedures. A range of intermediate annealing treatments between 1750°F and 2250°F (955°C to 1230°C) were explored for the alloys in question, using materials cold-worked to varying degrees.

An example of the typical behavior observed for materials given 40% prior cold reduction is presented in Figure 12 and Table 7. From the data plotted in Figure 12, it is readily apparent that the materials display significantly different responses to post-cold-work annealing. Although the yield strengths of the materials in the as-cold-worked condition all lie in the narrow

range of about 158 to 178 Ksi (1090 to 1225 MPa), the annealing temperature required to reduce the yield strength to, for example, 80 Ksi (550 MPa) varies from about 1750°F (955°C) for alloy S to about 2075°F (1135°C) for alloy No. 188.

This variation in yield strength as a function of alloy is a very important consideration in the formulation of intermediate annealing treatments or stress-relief treatments during fabrication. The ductility data presented in Table 7 show that it is possible to restore over 30% tensile elongation in all cases with, for example, a 1950°F (1065°C) anneal. However, the significantly higher resulting yield strengths for alloys No. 188, No. 230, and even No. 625, as compared to those for alloys S and X, could lead to serious limitations in subsequent forming operations.

Based upon these data, a set of guidelines is offered in Table 8 for heat-treatment of these alloys. The least demanding of the materials is alloy S. The most demanding, alloy No. 230. The low carbon content of alloy S allows for its ability to recrystallize to a reasonable grain size, with carbides in solution, at a lower temperature than most of the other alloys. On the other hand, the carbides present in alloy No. 230, which are tungsten-rich, are difficult to dissolve, hence the requirement for the higher solution-annealing temperature in this material. This sluggish dissolu-

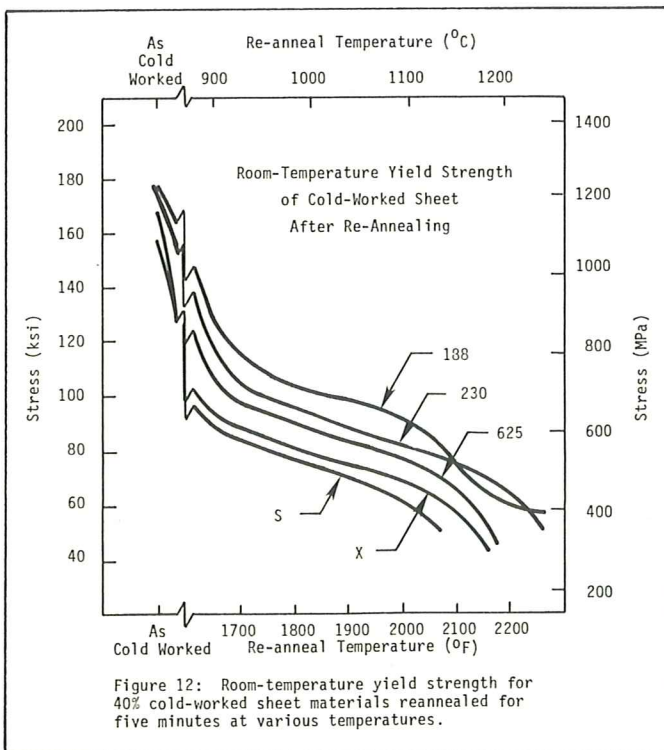


Table 8  
Guidelines for Alloy Heat Treatment

Alloy	Minimum Intermediate Anneal Temperature		Nominal Solution Heat Treatment Range	
	°F	°C	°F	°C
S	1750	955	1900-2100	1040-1150
X	1850	1010	2100-2200	1150-1205
625	1850	1010	2000-2100	1095-1150
188	2050	1120	2100-2200	1150-1205
230	2050	1120	2150-2250	1175-1230

tion is illustrated quite dramatically by the data in Table 9, which shows the effect of prolonged exposure at 2200°F (1205°C) upon the grain size of plate samples for alloys No. 230, No. 188 and X.

### Welding & Brazing

The joinability of the newer materials discussed here is almost self-evident from the complex welded and brazed components pictured in Figures 8 and 9. An attempt has been made, however, to develop a more quantitative appreciation, at least in terms of weldments, for the properties of the new and more established materials.

Table 9

Exposure Temperature		Grain Size of Plate Exposed for 24 Hours		
°F	°C	Alloy No. 230	Alloy No. 188	Alloy X
2150	1175	5 - 7	5 - 6	4 - 6-1/2
2200	1205	5 - 7	0 - 1	00 - 0

The welding and brazing practices employed successfully for alloy No. 230 and alloy S do not differ significantly from those used for alloy X or alloy No. 188. Post-weld heat-treatment is not required for these alloys. Pre-weld heat-treatment is required in the case of repair-welding of alloy X, alloy No. 188, and in some cases alloy No. 625 components after long-time service. This is not believed to be necessary in the case of either alloy S or alloy No. 230.

The room-temperature mechanical properties of all-weld-metal deposits, built-up by welding pieces of the same alloy plate together in a "cruciform", are given in Table 10 for gas tungsten arc weldments and in Table 11 for gas metal arc weldments. Particularly good strength and ductility combinations are notable for all of the alloys, with the possible exception of alloy X. Although these deposits have yet to be examined metallographically, the high ductility is a good indication of the absence of microfissuring and embrittling phases in the weld metal.

Typical gas tungsten arc welded room-temperature transverse tensile properties for sheet are

Table 10

Gas Tungsten Arc All-Weld-Metal Room Temperature Tensile Properties

Alloy	UTS		0.2% Y. S.		Elongation %
	ksi	MPa	ksi	MPa	
230	125.1	865	84.9	585	46.7
188	124.5	860	81.4	560	46.2
625	115.1	795	71.2	490	45.5
X	111.4	770	73.6	505	25.7
S	111.0	765	69.6	480	51.6

Table 11

Gas Metal Arc All-Weld-Metal Room Temperature Tensile Properties

Alloy	UTS		0.2% Y. S.		Elongation %
	ksi	MPa	ksi	MPa	
188	119.0	820	76.5	525	49.1
S	114.0	785	71.8	495	44.5
230	113.9	785	71.0	490	48.2
X	105.5	725	66.4	460	36.1

given in Table 12. All five materials exhibit good ductility, indicative of no heat-affected-zone cracking or embrittlement.

Table 12

Gas Tungsten Arc Welded Room Temperature Transverse Tensile Properties for Sheet

Alloy	UTS		0.2% Y. S.		Elongation %
	ksi	MPa	ksi	MPa	
188	140.5	970	66.8	460	50.5
625	134.8	930	68.7	475	46.7
230	128.7	885	54.9	380	46.4
X	110.3	760	51.6	355	45.6
S	104.8	725	51.4	355	45.1

### SUMMARY

The design and performance characteristics, together with the fabrication characteristics, of two newer solid-solution-strengthened superalloys, HAYNES alloy No. 230 and HASTELLOY alloy S, have been described. It has been shown that these alloys exhibit specific performance advantages over more traditional solution-strengthened superalloys, but maintain fabrication capabilities well within the experience curve for the more established alloys. Among the property advantages exhibited by these alloys are significantly better thermal stability, environment-resistance, and, in some cases, strength.

### REFERENCES

1. D. P. Moon, R. C. Simon, and R. J. Favor, "The Elevated-Temperature Properties of Selected Superalloys", ASTM Data Series DS 7-51, July, 1968, pp. 163-172.
2. O. F. Kimball, W. R. Pieren, and D. I. Roberts, "Effects of Elevated Temperature Aging on the Mechanical Properties and Ductility of Ni-Cr-Mo-Cb Alloy No. 625", Gulf GA-A12683, October, 1973.
3. M. F. Rothman, "Oxidation Resistance of Gas Turbine Combustion Materials", International Gas Turbine Conference, Houston, Texas, March, 1985, Paper No. 85-GT-10.